JOURNAL
OF THE AMERICAN CHEMICAL SOCIETY

VOLUME 98, NUMBER 23 NOVEMBER 10, 1976

# Structure and Reactivity of the Hypervalent Phosphoranyl Radicals

**James M. Howell*[1a] and John F. Olsen[1b]**

*Contribution from the Departments of Chemistry, Brooklyn College, City University of New York, Brooklyn, New York 11210, and Staten Island Community College, City University of New York, Staten Island, New York 10301.*
*Received November 21, 1975*

**Abstract:** Various optimized geometries are calculated for the $PH_4$ radical using the unrestricted Hartree-Fock method within an 4-31G basis set. The effect of d orbitals was also investigated. The $C_{2v}$ form resembling a trigonal bipyramidal structure with missing equatorial substituent (TBP-e) was taken as the $PH_4$ structure of minimum energy. The form of the orbitals and their energy variation with geometry are explored with a correlation diagram using the tetrahedral geometry as a starting point. The lower energy of the TBP-e geometry is attributed to a second-order Jahn-Teller type mixing. The relationship of the 9 valence electron $PH_4$ radical to 8 electron $PH_4^+$ and 10 electron $SH_4$ systems is discussed. Physical mechanistic pathways for ligand scrambling are found to have higher energy barriers (>15 kcal/mol) than for phosphoranes (2 kcal/mol). A potential surface for $PH_3 + H \rightarrow PH_4$ indicates a preferred attack where the incoming H enters an axial position. Optimized structures for the $PH_nF_{4-n}$ radicals appear qualitatively similar to $PH_4$. Calculated spin densities are correlated with experimental data.

The study[2-22] of the pentacovalent phosphorus, $PX_5$, systems (phosphoranes) has included bonding, molecular geometry, and ligand scrambling from physical mechanistic and permutational points of view. Both theoretical calculations[15-21] and experiments[22] indicate that the ligands in these $PX_5$ compounds are mobile with activation barriers on the order of 5 kcal/mol or less for the permutational processes. All these studies leave no doubt that the geometry of most five coordinate phosphorus is that of a trigonal bipyramid (TBP).

When one moves from the pentavalent phosphoranes to the tetravalent phosphoranyl radicals ($\cdot PY_4$) the picture of bonding and permutational isomerization becomes somewhat clouded. Phosphoranyl radicals have been identified[23] by ESR spectroscopy as intermediates in the reactions of certain radicals with trivalent P compounds, viz., $X\cdot + PY_3 \rightarrow XPY_3$, and also from P–X homolysis or abstractions involving phosphoranes, $R_4PX \rightarrow R_4P\cdot + X\cdot$ (where X = H or halogen). Most ESR studies agree that the $\cdot PH_4$ species can be thought of as being similar to pentacovalent phosphoranes with the odd electron acting as a sort of phantom ligand. Further, these studies suggest that the geometry of the $\cdot PY_4$ species can be viewed as distorted TBP with two distinct types of ligand sites, axial and equatorial.[24-29] Several chemical studies also support the intermediacy of $\cdot PY_4$ radicals.[23,30] Recent ESR studies on the simplest phosphoranyl radical $\cdot PH_4$ have presented conflicting ideas concerning the structure of the radical.[31,32] In addition to the conflicts associated with the structure of $\cdot PH_4$ there is uncertainty of a chemical[30d,33] and theoretical[34,35] nature concerning the permutational stability of the phosphoranyl system. For example, the ESR work of Krusic[25] is interpreted as indicating a rapid interchange of ligand sites. On the other hand Bentrude's competitive experiments[30] involving $\beta$ scission indicate slow interchange. Finally, chemical evidence[36] has demonstrated that the X· radical in the reaction $X\cdot + PY_3$ does not enter into the TBP in a configurationally random way but rather it has been presumed to enter axially.[25,28,29]

The objectives of the present study then are first to shed some light on the electronic structure of $\cdot PH_4$ and its preferred geometry. We also examine the energetic cost of excursions from the minimum energy geometry, i.e., the energetics of different mechanistic possibilities for site interchange in $\cdot PH_4$. We explore the potential energy surface for the reaction between $PH_3$ and H· in the hope of answering the question on the preferred direction of attack by radical species. The calculations were performed both with and without d functions on phosphorus so that the importance of d orbitals in the bonding of these compounds can be evaluated.[37] Last, we look at the effects of fluorine substitution in the $PH_nF_{4-n}$ radicals.

## Quantum Chemical Methods

The calculations reported here were carried out at two levels of approximation. On the one hand, we have used the split-valence 4-31G basis set of the GAUSSIAN 70 program system[38] for the full optimization of each $\cdot PH_4$ and $\cdot PH_nF_{4-n}$ structure. This involves the variation of all bond lengths and bond angles, subject to assumed symmetry constraints, until variation of 0.01 Å and 1° lead to no further lowering of the total energy. The 4-31G geometry is then used as the basis for a single cal-

**Table I.** Optimized Geometric Parameters for the Species $PH_4$, $SH_4$, $PF_4$, $PH_2F_2$, and $SH_2F_2$

| Molecule | Bond length, Å | | Bond angle, deg | | Method | Ref |
|---|---|---|---|---|---|---|
| | $r_a$[c] | $r_e$[c] | $\alpha$[c] | $\beta$[c] | | |
| $PH_4$ | 1.42[a] | 1.42[a] | 198 | 97 | CNDO | 31 |
| | 1.58 | 1.51 | 180[b] | 120[b] | CNDO | 42 |
| | 1.53 | 1.45 | 210 | 98 | INDO | 43 |
| | 1.64 | 1.42 | 187.5 | 97.0 | 4-31G | Present work |
| $SH_4$ | 1.70 | 1.35 | 168.2 | 105.6 | Ab initio | 44 |
| | 1.374 | 1.374 | 163.7 | 163.7 | Ab initio | 45 |
| $PF_4$ | 1.89 | 1.80 | 202 | 96 | INDO | 43 |
| | 1.71 | 1.61 | 193 | 101 | 4-31G | Present work |
| $PH_2F_2$ ($F_{apical}$) | 1.74 | 1.40 | 195 | 107 | 4-31G | Present work |
| $SH_2F_2$ ($F_{apical}$) | 1.73 | 1.33 | 167 | 101 | Ab initio | 45 |

[a] Assumed bond lengths. [b] Assumed bond angles. [c] $r_a$ and $r_e$ are the apical and equatorial ligand central atom bond distances and $\alpha$ and $\beta$ are the corresponding angles defined in Figure 1.

culation on $\cdot PH_4$ at the second level of approximation where d functions were allowed for the phosphorus basis set. For $PH_4$ the full basis set consisted of 58 primitive Gaussian functions with a d exponent on phosphorus of 0.36, contracted to 27 basis functions.[39b] The SCF calculations with d functions were carried out with the POLYATOM program.[40] Since the calculations reported here are concerned with odd electron species, the open-shell states were computed using the unrestricted Hartree–Fock procedure.[41]

### Geometry Study of $PH_4$

As a starting point in our discussion of geometry we refer to the optimized $D_{3h}$ (**1**) and $C_{4v}$ (**2**) geometries of $PH_5$. The

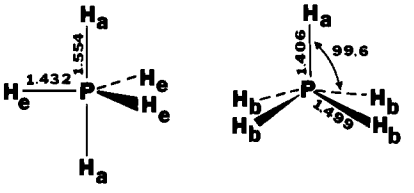


1 2

$D_{3h}$ structure has an energy of −343.025 24 hartrees in our 4-31G calculations (without d) while the energy of **2** (the oft studied transition state geometry of the Berry pseudorotation) is only 1.8 kcal/mol higher. (This value is typical[15-20] of the calculated barriers for site interchange in $PX_5$ phosphoranes.) From these two structures we may generate four radicals by removing a single hydrogen from one of the four distinct sites in **1** or **2**.

The energies (relative to **2b** at −342.491 42 hartrees) of the four different radicals are given below where, for example, **1e** is the radical produced by removing an equatorial hydrogen from **1**: **1e** 1.6 kcal/mol, **1a** 21.9, **2a** 46.2, **2b** (0.0).

Fragments **2b**, with a missing basal hydrogen, and **1e** are very close in energy and further geometry optimization is necessary. Structures **3–6** give the optimized geometries for

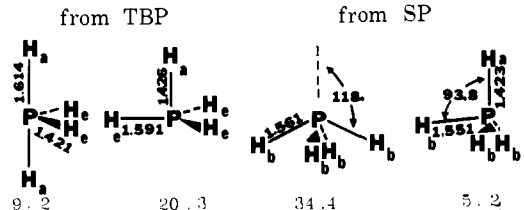


the fragment radicals just discussed. We have optimized those geometric parameters indicated and the energies are reported relative to the $C_{2v}$ geometry (vide infra) of minimum energy. (Values in parentheses refer to relative energies where d orbitals are included in the basis set.) We also show in **7** and **8**

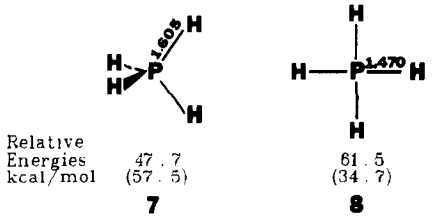


the optimized structures and energies for optimized tetrahedral and square-planar $\cdot PH_4$.

Structure **6**, derived from the square pyramid, may be regarded as a deformed trigonal-bipyramid fragment where the "equatorial" ligands are $H_a$ and the leftmost $H_b$. The completely optimized $C_{2v}$ structure is given in **9** (energy =

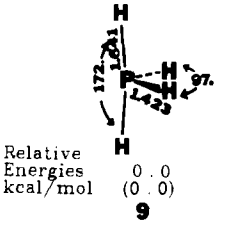


−342.504 76 hartrees without d and −342.562 97 with d). Table I compares our optimized geometry with the conclusions of other investigations. We use TBP-e as a notation for a trigonal bipyramid radical with a missing equatorial ligand such as **1e**, **3**, or **9**. The meaning of TBP-a, SP-b, or SP-a is similarly defined. In summary we find that the TBP-e form is substantially lower in energy than the TBP-a geometry. Further the SP-a geometry is high in energy while the SP-b is low and resembles the TBP-e. We take the $C_{2v}$ structure, **9**, as our reference structure. The inclusion of the set of 3d orbitals led to an optimized axial bond length of 1.566 Å for the TBP-e structure (−342.565 6 hartrees).

As may be seen from the energies reported above and also those of Table II the primary role of the d orbitals is to lower the total energy by a relatively constant amount. The orbital energies and their ordering agree well with those computed without d functions. The glaring exception being the square-planar structure where d orbitals are expected to participate to the greatest extent since the nodal structure of the singly occupied $1b_{1g}$ orbital allows for large 3d participation. The without-d 4-31G calculations yielded a $^2B_{1g}$ ground electronic state whereas the with-d calculation yielded an electronic configuration with the $1b_{1g}$ molecular orbital doubly occupied

**Table II.** Total and Valence Orbital Energies (Hartrees) for the Optimized $PH_4$ Fragments (3–9)

| | TBP-e $C_{2v}$ (9) | | | | TBP-e $C_{2v}$ (3) | | | | SP-b $C_s$ (6) | | |
|---|---|---|---|---|---|---|---|---|---|---|---|
| Sym- | α-MO's | | β-MO's | | α-MO's | | β-MO's | | Sym- | α-MO's | β-MO's |
| metry | No d GTF | d GTF | No d GTF | d GTF | No d GTF | d GTF | No d GTF | d GTF | metry | No d GTF | No d GTF |
| $4a_1$ | −0.893 | −0.868 | −0.879 | −0.848 | −0.893 | −0.872 | −0.873 | −0.843 | 5a′ | −0.896 | −0.874 |
| $2b_1$ | −0.581 | −0.563 | −0.487 | −0.478 | −0.587 | −0.568 | −0.494 | −0.487 | 2a″ | −0.603 | −0.512 |
| $2b_2$ | −0.541 | −0.534 | −0.539 | −0.533 | −0.575 | −0.567 | −0.568 | −0.564 | 6a′ | −0.528 | −0.520 |
| $5a_1$ | −0.490 | −0.487 | −0.433 | −0.433 | −0.449 | −0.448 | −0.391 | −0.392 | 7a′ | −0.486 | −0.437 |
| $6a_1$ | −0.303 | −0.312 | | | −0.312 | −0.319 | | | 8a′ | −0.289 | |
| Total energy = −342.504 76 (−342.562 97) | | | | | −342.490 08 (−342.550 78) | | | | −342.496 48 | | |

| | TBP-a $C_{3v}$ (4) | | | | SP-a $C_{4v}$ (5) | | | | | $T_d$ (7) | | |
|---|---|---|---|---|---|---|---|---|---|---|---|---|
| Sym- | α-MO's | | β-MO's | | Sym- | α-MO's | | β-MO's | | Sym- | α-MO's | β-MO's |
| metry | No d GTF | d GTF | No d GTF | d GTF | metry | No d GTF | d GTF | No d GTF | d GTF | metry | No d GTF | No d GTF |
| $4a_1$ | −0.856 | −0.864 | −0.878 | −0.845 | $4a_1$ | −0.833 | −0.857 | −0.877 | −0.838 | $3a_1$ | −0.869 | −0.857 |
| 2e′ | −0.557 | −0.546 | −0.495 | −0.494 | 2e | −0.588 | −0.575 | −0.494 | −0.480 | $2t_2$ | −0.540 | −0.492 |
| $5a_2'$ | −0.525 | −0.521 | −0.481 | −0.475 | $5a_1$ | −0.383 | −0.381 | −0.394 | −0.370 | $4a_1$ | −0.175 | |
| $6a_1'$ | −0.239 | −0.244 | | | $6a_1$ | −0.366 | −0.356 | | | | | |
| Total energy = −342.472 24 (−342.534 27) | | | | | −342.449 97 (−342.506 99) | | | | | −342.428 73 | | |

| | $D_{4h}$ (8) | | | |
|---|---|---|---|---|
| | α-MO's | | β-MO's | |
| Symmetry | No d GTF | d GTF | No d GTF | d GTF |
| $3a_{1g}$ | −0.867 | −0.900 | −0.848 | −0.823 |
| $2e_u$ | −0.612 | −0.577 | −0.519 | −0.568 |
| $1b_{1g}$ | −0.386 | −0.328 | | −0.341 |
| $2a_{2u}$ | −0.289 | −0.398 | −0.307 | |
| Total energy = −342.406 86 (−342.507 75) | | | | |

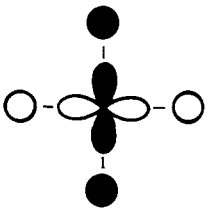

**$1b_{1g}$**

for an overall $^2A_{2u}$ symmetry. In addition, the relative energy of this fragment is substantially lowered by the presence of d functions, lower in fact than the $C_{4v}$ geometry (SP-a). We will return to these energetic considerations below. Suffice it to say that for the most part d orbitals have mathematical but not stereochemical significance.[37]

### Electronic Structure of $PH_4$

In the structures **3–8** we have shown several of the geometric possibilities for an $AH_4$ species. In this section we attempt to rationalize the energy differences between the TBP-e, TBP-a, and SP-a geometries of $\cdot PH_4$ and then to provide a relationship to other systems such as $PH_4^+$ or $SiH_4$ with one less electron and $SH_4$ or $PH_4^-$ with an additional electron. Figure 1 shows two correlation diagrams relating the calculated[46] orbital energies of the tetrahedral $\cdot PH_4$ in the center to those of the TBP-a ($C_{3v}$) geometry on the left and the SP-a ($C_{4v}$) geometry on the right which is reached via the TBP-e ($C_{2v}$) form. The geometric variable for the deformation toward a square pyramid is the H–P–H angle $\alpha$. As it is decreased from its initial tetrahedral value of 250.53 to 180° the $C_{2v}$ geometry resembles that of the TBP-e structures **3** and **9** finally reaching 109.47° and the $C_{4v}$ SP-a structure similar to **5**.

The forms of the orbitals for tetrahedral $\cdot PH_4$ are the same as those of other well known valence shell isoelectronic systems such as $CH_4$. The lowest lying valence shell orbital, $3a_1$, is derived from the P 3s orbital bonding with the four hydrogen 1s orbitals. The next set is the triply degenerate $2t_2$ set, the bonding combination of the P 3p orbitals, and the symmetry adapted combinations of the H 1s orbitals. In our calculations on the tetrahedral $\cdot PH_4$ the radical or singly occupied orbital is the $4a_1$ orbital wherein the P 3s is antibonding to all of the H 1s orbitals.

As $\alpha$ is decreased the symmetry is reduced from $T_d$ to $C_{2v}$ and then finally reaches $C_{4v}$. The symmetry of the orbitals matches up as follows

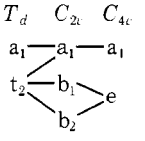


The energies of the valence shell molecular orbitals behave as expected from overlap considerations. In $C_{2v}$ symmetry the $4a_1$ orbital is relatively insensitive to changes in $\alpha$. With the threefold degeneracy of the $t_2$ set split the lowest orbital, $2b_1$, derived from P $3p_x$ orbital passes through a shallow minimum as the hydrogen 1s orbitals pass through the $x$ axis. On the other hand the $2b_2$ orbital derived from the P $3p_y$ orbital maintains an unchanging overlap with the H 1s orbitals and its energy is nearly constant. The $5a_1$, derived from the P $3p_z$,

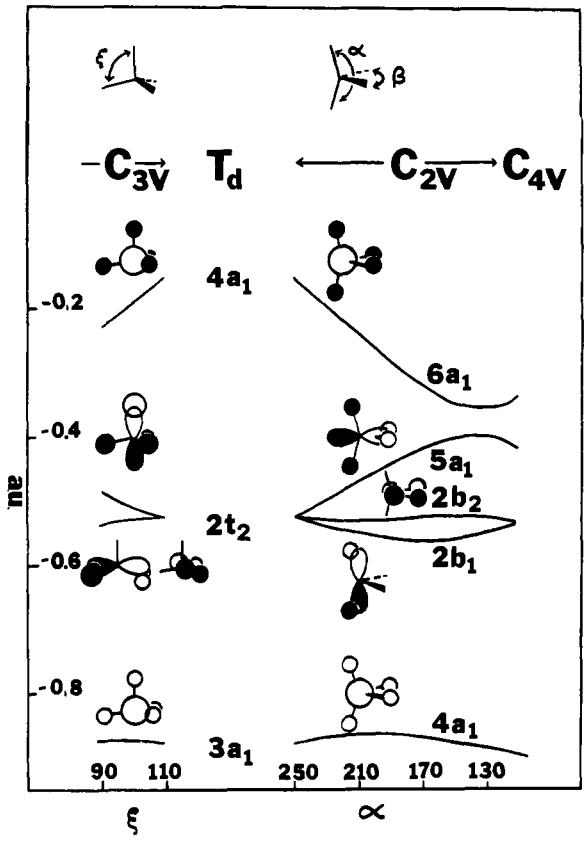


**Figure 1.** A correlation diagram for deformations of the $PH_4$ radical calculated holding all P-H at 1.558 Å. In the center are the orbital energies in the tetrahedral geometry. The angle $\alpha$ is decreased in moving to the right until finally the $C_{4v}$ geometry of the square pyramid is reached. In moving from the center toward the left the angle $\xi$ is decreased and the geometry is $C_{3v}$.

orbital moves strongly upward as the overlap with the moving H 1s orbitals drops to zero at $\alpha = 180°$ and becomes antibonding at $\alpha$ less than 180°. An avoided crossing occurs with the $6a_1$ which is dropping in energy. Since the behavior of the singly occupied $6a_1$ orbital is critical to the geometry and energetics of the molecule we will examine the make-up of the orbital in some detail.

The $3t_2$ set of virtual orbitals is triply degenerate allowing us to take whatever linear combination is convenient in discussing distortions to the TBP-e or TBP-a geometries. Scheme I shows the mixing of the $z$ oriented member of the tetrahedral $3t_2$ set of orbitals into the $4a_1$ orbital that occurs when $\alpha$ is decreased and $C_{2v}$ symmetry prevails. In the resultant orbital there is a buildup of density at the axial position and a decrease at the equatorial. Overall charges are $H_a = -0.062$ and $H_e = -0.014$ for structure **9**. As expected this leads to the preference of an electronegative substituent for the axial site in the TBP-e geometry (vide infra). The same sort of considerations hold for the distortion leading to the $C_{3v}$ TBP-a as shown in Scheme II where we are making use of an alternative linear combination of the $3t_2$ orbitals. There is a pronounced weakening of the P-$H_a$ bonds in the TBP-e form and of the P-$H_e$ bonds in TBP-a. The bond lengths are shown in **2** and **3**.

As the symmetry is reduced from $T_d$ to $C_{2v}$ (or $C_{3v}$) the $4a_1$ orbital was stabilized by mixing with the appropriate $3t_2$ virtual orbital of higher energy ($T_d$ notation). We estimate the extent of stabilization by a simple perturbation calculation. We regard the coefficients of the $4a_1$ and the appropriate $3t_2$ orbital of $T_d$ geometry as being frozen while we deform the molecule to the TBP-e or TBP-a geometry. The stabilization is then estimated as being related to the overlap of the frozen molecular orbitals.

Scheme I

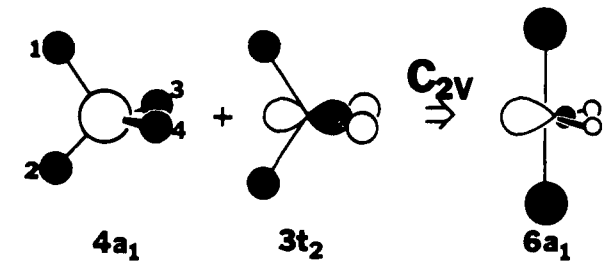


Scheme II

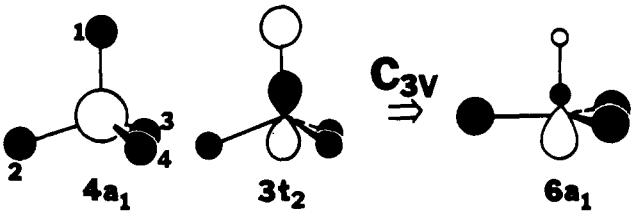


The $4a_1$ orbital ($T_d$ notation) is represented by

$$\phi(4a_1) = c_1 s + c_2(h_1 + h_2 + h_3 + h_4)/2$$

and the appropriate member of the $3t_2$ set shown in Scheme I for the $C_{2v}$ motion is

$$\phi(3t_2) = d_1 p + d_2(h_1 + h_2 - h_3 - h_4)/2$$

and for the $C_{3v}$

$$\phi'(3t_2) = d_1 p + d_2(h_2 + h_3 + h_4 - 3h_1)/\sqrt{12}$$

where $s$ and $p$ refer to phosphorus 3s and 3p orbitals and $h_1$, etc., are the hydrogen 1s orbitals appearing in normalized symmetry adapted combinations (assuming zero overlap). The overlap integrals are readily calculated for the TBP-e structure:

$$S_e \equiv \int \phi(4a_1)\phi(3t_2)\, dV = c_2 d_1 S \cos(\beta/2)$$

and for the TBP-a structure

$$S_a \equiv \int \phi(4a_1)\phi'(3t_2)\, dV = c_2 d_2 S/2$$

where $S$ is the overlap between a H 1s orbital and a P 3p orbital directed along the internuclear P-H axis. $\beta$ is the angle defined in Figure 1. Using $\beta = 109.47°$ $S_e$ turns out to be 15% greater than $S_a$. (In our optimized structure, **9**, $\beta$ is 97° and $S_e$ some 33% larger than $S_a$.) Clearly, the mixing and resultant stabilization should be greater for the TBP-e form than the TBP-a. We find that within our calculations the coefficient of the diffuse component of the phosphorus 3p orbital is 0.444 for the singly occupied orbital of TBP-e structure, **9**, and 0.405 for the corresponding $6a_1$ orbital of the TBP-a form, **4**. Pearson[47] and Bartell and Gavin[48] have given similar "second-order Jahn-Teller" arguments for $SF_4$. Bartell has also presented pictorial arguments[6b] concerning such distortions.

$SH_4$, possessing one more electron than $\cdot PH_4$, has been calculated ab initio and the results are presented in Table I. The optimized $C_{2v}$ structure of $SH_4$ computed by Schwenzer and Schaefer[44] is found to be a TBP-e except that it is distorted toward a square-pyramidal geometry in contrast to the distortion toward $D_{2d}$ in $PH_4$ ($\alpha = 168.2°$, $\beta = 105.6°$).

Gleiter and Veillard[45] using a basis set of similar quality to that of Schwenzer and Schaefer find the optimum structure for $SH_4$ to be a square pyramid ($\alpha = \beta = 163.7°$). Since a relatively small change in basis set causes the optimum form to change from $C_{4v}$ to $C_{2v}$ the energy difference between the two geometries must be small for $SH_4$ whereas for $\cdot PH_4$ it is found to be substantial in our calculations. The situation is

easily rationalized however by means of the correlation diagram in Figure 1.

An eight valence electron problem such as $SiH_4$ or $PH_4^+$ with $5a_1$ ($C_{2v}$ notation) as the highest occupied orbital should clearly prefer the tetrahederal geometry whereas the hypervalent 10 electron problem should prefer geometries with $\alpha$ less than 180° due to the rapidly falling $6a_1$ orbital. Thus we might expect the $C_{4v}$ form as being the optimum geometry or at least a $C_{2v}$ form with $\alpha$ less than 180°.

The maximum that occurs in the $5a_1$ curve when $\alpha$ is about 135° suggests that the $C_{4v}$ structure might represent a metastable geometry for 9 valence electron systems. This would make the $C_{4v}$ geometry an intermediate rather than a transition state for the Berry process. However, the total energy of our calculations monotonically increases as $\alpha$ goes from 180 to 110° in Figure 1. The valence molecular orbital energies of the optimized geometries are given in Table II.

## Mechanisms of Ligand Scrambling

As mentioned in the introductory section there is some uncertainty about the size of the energy barrier to the ligand scrambling processes of phosphoranyl radicals. For phosphoranes, $PX_5$, where the energy barrier is low, there have been two widely considered mechanisms: the Berry pseudorotation[14] and the turnstile mechanism.[15] We first examine the Berry-like process which is usually assumed to involve a square-pyramidal transition state.

Scheme III allows the radical lobe to occupy the apical position of the square-pyramidal transition state, **5**, which was calculated (vide supra) to lie some 34 kcal/mol above the optimized $C_{2v}$ structure. We have also considered the possibility that the $C_{4v}$ transition state may be avoided in the pathway of Scheme III, possibly allowing for a lower energy transition state. Toward this end we have calculated the energy as a function of the angles $\alpha$ and $\beta$ defined as in Figure 1 on a two-dimensional potential surface. $C_{2v}$ symmetry was maintained and for each pair of $\alpha$ and $\beta$ values the bond lengths were optimized. The energy barrier was found to be about 34 kcal/mol.

Scheme IV is a double pseudorotation designed to keep the radical lobe out of the apical position in the square-pyramid geometries. In the first Berry pseudorotation ligand **4** is held fixed as the pivotal substituent and ligand **1** is pivotal for the second Berry process. The high-energy point is likely to be the $C_{3v}$ structure **4** which is about 20 kcal/mol above the optimized $C_{2v}$ form.

The turnstile mechanism is an alternative pathway for ligand scrambling which has been found in theoretical studies[15-20] of $PX_5$ systems to be higher energy than the Berry process. However, in the tetracoordinate radical the turnstile process deserves fresh consideration. Ugi and Ramirez[15] formulated the turnstile process for phosphoranes as involving a group of three ligands rotating against the remaining group of two. It is usually assumed that the group of three ligands (one axial and two equatorial) deform slightly so as to have a local threefold axis coincident with the local twofold axis for the P and the two remaining ligands. For the phosphoranyl radical we may envisage the phantom ligand of the radical lobe as being included in either the trio or the duo. Scheme V places the radical lobe in the duo.

As with Scheme IV we expect that Scheme V is likely to be a high energy process due to the 60° structure which resembles the TBP-a geometry. Figure 2 shows a potential surface calculated for the rotational motion holding all P-H distances at 1.558 Å. The energy is given as a function of rotation when a local $C_{3v}$ symmetry is forced upon the trio of hydrogens. The high point in this curve is some 15 kcal/mol above the optimum TBP-e form. This is also the energy of the optimized $C_{3v}$ structure (similar to **4**) within the equal bond length restriction.

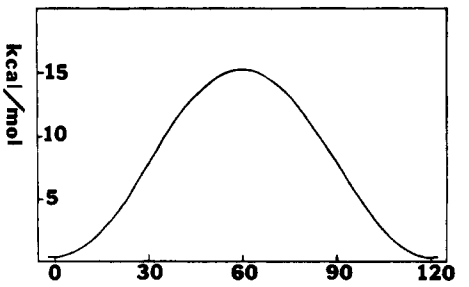


**Figure 2.** A potential surface for a turnstile ligand scrambling process in $\cdot PH_4$ with the radical lobe in the duo. See Scheme V. All P-H distances were held at 1.558 Å. A local threefold symmetry was forced upon the trio.

Scheme III

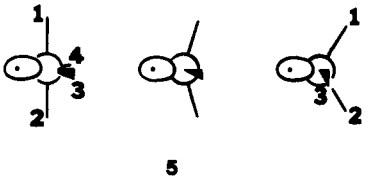


Scheme IV

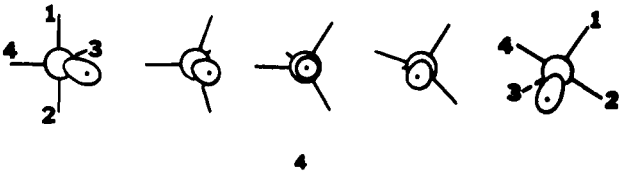


Scheme V

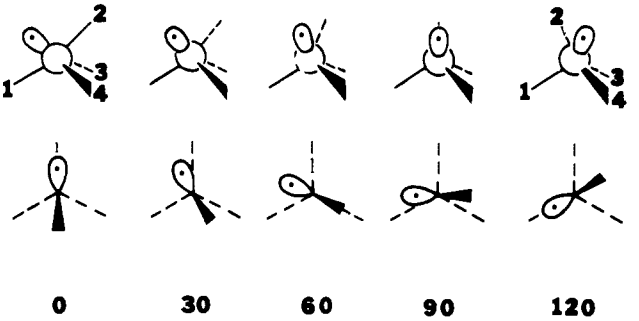


Scheme VI

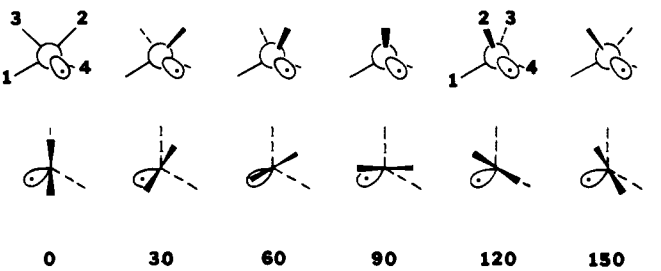


In Scheme VI the radical lobe is part of the trio at the bottom of each structure. The changing of $\phi$ from 0 to 60° generates a geometry similar to the TBP-a form. Further rotation to $\phi = 120°$ produces a structure equivalent to $\phi = 0$ and resembling the TBP-e. Further rotation to $\phi = 150$ (occurring also at $\phi = -30°$) produces a form resembling the SP-a geometry which is high in energy (see structure **5**). We show in

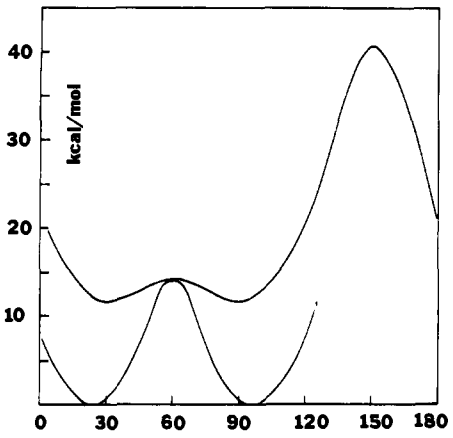


Figure 3. Two potential surfaces for the turnstile mechanism with the radical lobe in the trio. See Scheme VI. All P-H distances were held at 1.558 Å. The upper curve was calculated forcing a local twofold symmetry on the duo and a local threefold on the trio. The two- and threefold axes were coincident. In the lower curve the angular restrictions were relaxed.

Figure 3 two curves for the $\phi$ cut thru the potential hypersurface. The higher energy curve was calculated with the constraint that the angles made by the P–H bonds of the trio and the $z$ axis were kept equal to each other. Similarly, the angles between bonds to the duo hydrogens and the $z$ axis were maintained to be equal. At each value of $\phi$ the two sets of bond angles were optimized.

The energy of the upper curve does not fall to zero, corresponding to that of the optimized TBP-e form. In the lower curve segment we remove the equal bond angle constraint and have optimized for a given choice of $\phi$ each of the four angles made by the P–H bonds with the $z$ axis. The curve falls to the zero energy at $\phi$ = 25 and 95°, not at 0 and 120°. This is due to the optimum bond angles within the TBP-e structure not being 90 and 120°. See structure **9** for the overall $C_{2v}$ minimum. However, the important point is that the additional optimization has not produced any further lowering of the energy barrier. Last, we note that the curve is symmetric about $\phi$ = 60, 150, 240, and 330°.

The processes of Schemes IV–VI are all quite similar. The energy barrier is calculated to be 14–15 kcal/mol in each case due to the presence of a TBP-a like form at or near the transition state. Furthermore, in each case the same permutation of ligands ($M_4$ in Musher's notation[49]) occurs. In particular, the H2–P–H4 angles opens up from about 90°, as in **10**, to finally reach a value close to 180°.

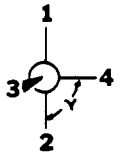


**10**

In order to further explore and characterize the reaction pathway we have approached the problem from a different viewpoint using the H2–P–H4 angle, $\gamma$, as the geometric variable. The cut through the five-dimensional hypersurface was calculated by optimizing the four remaining degrees of freedom for each choice of $\gamma$. The resultant pinwheel motion is shown in (1).

Atoms 1, 2, 4, and the phosphorus all remain nearly coplanar while atom 3 moves to the right. The motions of Schemes IV–VI are all of this pinwheel type. The transition state of (1) is calculated to be a slightly distorted TBP-a and, not surprisingly, is calculated to have an energy within 1 kcal/mol of

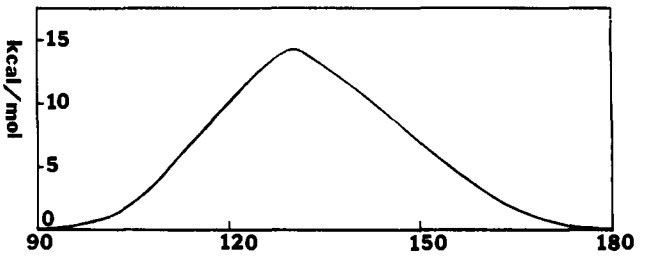


Figure 4. A potential surface for $\cdot PH_4$ ligand scrambling where the angle between an axial and equatorial hydrogen is forced open from 90 to 180° (horizontal axis). The bond lengths were kept at 1.558 Å. The overall motions are shown in eq 1.

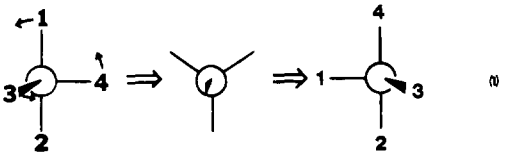


(1)

the optimized $C_{3v}$ TBP-a. The potential energy curve is shown in Figure 4. It is important to note that the calculations just described were performed by holding all P–H distances at 1.558 Å. If the bond lengths are optimized then the TBP-a fragment **4** is about 20 kcal/mol above the $C_{2v}$ minimum **9.**

We should additionally note that the potential surface cut shown in Figure 4 should provide the same barrier as the lower curve of Figure 3. Both series of calculations involved optimizations of four angular degrees of freedom. These along with the reaction coordinate comprise the complete set of geometric variables for the nontranslating, nonrotating molecule with equal bond lengths.

In summary we find that for the scrambling pathways considered the energy barriers are likely to be significantly higher than is the case with phosphoranes (1.8 kcal/mol for $PH_5$) due to a transition state resembling the TBP-a geometry. While our calculations indicate a high barrier to rearrangement we must draw the readers' attention to problems, encountered in the $PH_4 \rightarrow PH_3 + H$ potential surface, described in the next section. In particular, we note that the stretching of one axial bond (a low energy process, vide infra) and the adoption of $C_{3v}$ symmetry could provide a low energy scrambling process.

### $PH_3 + H$ Potential Surface

We have calculated a cut through the potential surface for the reaction of $PH_3 + H \rightarrow PH_4\cdot$ using a 4-31G basis set. The coordinate system used to describe the approach of H to $PH_3$ is shown in **11.** The angle between the $z$ axis and the vector to

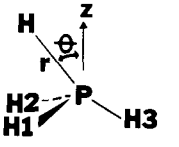


**11**

the incoming H is $\theta$ and the length is $r$. The incoming atom H and H3 are restrained to the plane of the page. In our calculations we held the angle of the P–H3 bond fixed at $\theta$ = 288.4° and kept H1 and H2 as mirror images of each other. For each choice of $r$ and $\theta$ we optimized the remaining geometric degrees of freedom. For large values of $r$ the $PH_3$ fragment maintained its identity and suffered only small geometric reorganization. For closer approaches the $PH_3$ underwent some distortion.

The potential surface is shown in Figure 5 where the energies are given relative to the sum of isolated $PH_3 + H\cdot$. We calculate an energy barrier of zero for the fragmentation of $PH_4$ to

$PH_3 + H\cdot$, i.e., it is a wholly downhill process with the $PH_3 + H\cdot$ lying some 13 kcal/mol lower than $PH_4\cdot$. This contradicts experimental findings where $\cdot PH_4$ has been observed by various techniques.[32] Consequently, we must regard our potential surface with some skepticism. Configuration interaction calculations might serve to produce a barrier to the fragmentation. However, we believe that the surface is probably reliable for indicating the preferred angles of approach.

We wish to note several particular approaches of the H atom to $PH_3$ in **12**.

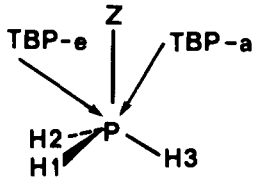


**12**

An attack along the $z$ axis would lead to geometries resembling the $C_{3v}$ structure **4**, TBP-a, with the incoming H occupying the short bond length axial position. Reference to Figure 5 indicates this is a relatively high energy pathway. The approach labeled TBP-a of **12** might also lead to a structure resembling the TBP-a, **4**, with H3 occupying the axial site. The incoming H would occupy a longer length equatorial (or basal) position. The potential surface favors this approach over the $C_{3v}$ axial approach as indicated by the inward bulging of the contours. However, the clearly favored angle of attack is the one labeled TBP-e leading to **3** (or **9**). Here the incoming H and H3 will occupy the "axial" sites. As the H atom approaches the $PH_3$ along the TBP-e pathway ($\theta \approx 52°$) the P-H3 bond length increases as would be expected. We note that the TBP-2 and TBP-e approaches are interconverted by a 60° rotation of the $PH_3$ around its $C_3$ axis.

The potential surface was repeated performing a single calculation with d orbitals utilizing the s,p-only optimized geometries. The effect of the d orbitals was to lower each point by 32–37 kcal/mol not changing our conclusion that the incoming H comes directly into an "axial" site.

### The Fluorinated Phosphoranyl Radicals

It was decided to study the effects fluorine substitution has on the electronic structure of the radicals. We first examined the $\cdot PF_4$ radical in geometries analogous to those considered for $\cdot PH_4$. Due to the presence of the four fluorines it was decided initially to employ the minimal STO-3G basis set for these calculations.[39a] The idealized fragments for $PF_4$ are presented in structures **13–18.**

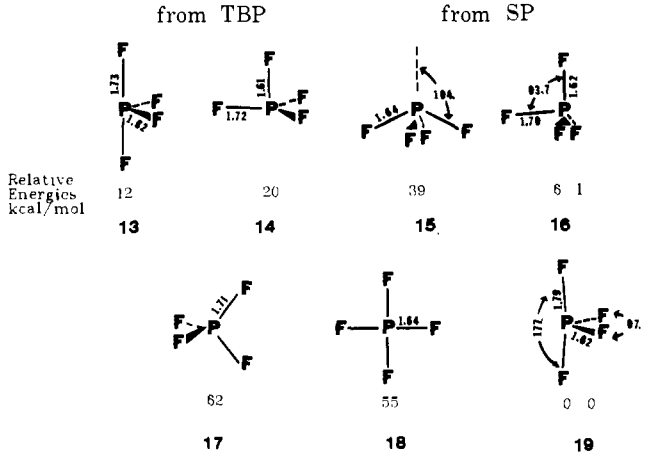


The overall $C_{2v}$ optimized structure for $\cdot PF_4$ is shown in **19** and comparison with **7** shows that complete fluoro substitution

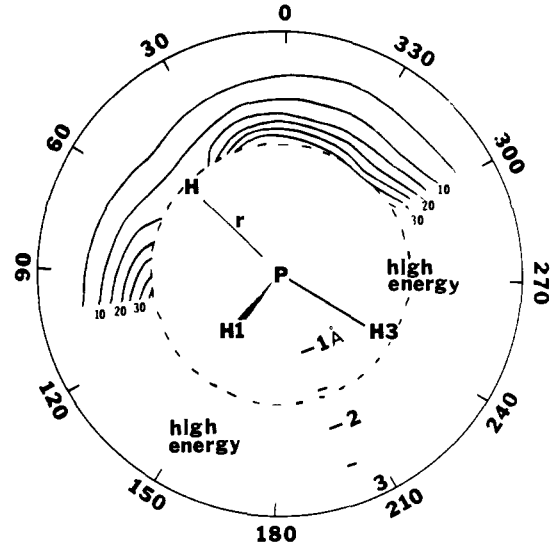


**Figure 5.** A portion of the potential surface for the reaction $PH_3 + H \rightarrow \cdot PH_4$ determined for $r$ between 1.6 and 3.0 Å and $\theta$ 300 to 100°. H1 and H2 are mirror images with respect to the page. See **11** and **12.** The P-H3 bond was kept in the plane of the page along the $\theta = 238.4°$ ray. The incoming H was kept in the plane of the page. For each choice of $r$ and $\theta$ the remaining degrees of freedom were optimized. The contours are at 5-kcal/mol intervals with the outermost contour being at +5 kcal/mol with respect to the $PH_3 + H$. The $PH_3$ is shown in the geometry assumed for large values of $r$. The angular ranges indicated as "high energy" include contours of at least 30 kcal/mol.

has not significantly modified the bond angles and **19** is still best classified as a TBP-e fragment. The energies of the fragments **13–18** are given in kcal/mol relative to the minimum **19** (at −728.972 86 hartrees). As with $\cdot PH_4$ the fragment of the square pyramid with a basal fluorine missing (**16**) is the lowest in energy. However, examination of the bond angles indicates that, as with $\cdot PH_4$, it might better be classified as a distorted TBP fragment. The basic geometric and energetic trends as found for $PH_4$ also held true for $\cdot PF_4$.

Because of the problem inherent in comparing calculations using different basis sets and also the large spin contamination of the STO-3G wave functions it was decided to examine the $\cdot PH_nF_{4-n}$ radical species using again the extended 4-31G basis. The structures for the $PF_4$, $PF_3H$, and $PF_2H_2$ radicals are presented in **20–22** where we have optimized the bond

**20** **21** **22**

lengths and the angles shown. It is known[50] that the 4-31G method leads to bond lengths that are usually too short and we see that the 4-31G calculations (**20**) yield shorter bond lengths than the STO-3G (**19**). The apical angle is also found to be consistently smaller using 4-31G.

The energy of the optimized isomer of **22** with the hydrogens axial rather than equatorial is 19.7 kcal/mol higher in energy as might be expected from applying the apicophilicity rule found in pentacovalent phosphorus compounds. It might also be mentioned that the stability of the radicals should increase with increasing fluorine substitution assuming that we may correlate the stability order with the energy of the highest occupied molecular orbital: $PH_4$ (−0.303); $PH_2F_2$ (−0.421); $PHF_3$ (−0.450); $PF_4$ (−0.498 hartree).

Table II compares our calculated results on $PF_4$ with the

**Table III.** Mulliken Population Analyses for the Optimized $PH_nF_{4-n}$ Radicals

| Radical | | s orbital spin density | $\langle S^2 \rangle$ | Atomic populations |
|---|---|---|---|---|
| $PH_4$ (**9**) | P | 0.060 (0.069) | | 14.904 (15.14) |
| | $H_a$ | 0.545 (0.452) | 0.800 | 1.062 (1.04) |
| | $H_e$ | −0.032 (−0.040) | | 0.986 (0.890) |
| $PH_2F_2$ (**22**) | P | 0.241 | | 13.986 |
| | $F_a$ | −0.004 | 0.772 | 9.583 |
| | $H_e$ | −0.062 | | 0.924 |
| $PF_3H_e$ (**21**) | P | 0.264 | | 13.496 |
| | $F_a$ | −0.004 | 0.773 | 9.508 |
| | $F_e$ | 0.001 | | 9.583 |
| | H | −0.025 | | 0.905 |
| $PF_4$ (**20**) | P | 0.295 | | 12.862 |
| | $F_a$ | 0.008 | .778 | 9.508 |
| | $F_e$ | 0.00066 | | 9.561 |

**Table IV.** Experimental and Computed[a] Hyperfine Coupling Constants in the Fluorophosphoranyl Radicals

| | $^{31}P$ | | | Apical ligands | | | Equatorial ligands | | |
|---|---|---|---|---|---|---|---|---|---|
| Radical | Exptl[b] | INDO[b] | 4-31G[c] | Exptl | INDO | 4-31G | Exptl | INDO | 4-31G |
| $PF_4$ | 1322 | 569 | 1074 | 294 | 71 | 137 | 59.5 | 4 | 12 |
| $PF_3H_{eq}$ | 1031 | 609 | 961 | 225.2 | 79 | −68.4 | 38.5(F) | 5 | 17.1 |
| | | | | | | | 38.5(H) | 11 | −12.7 |
| $PH_2F_2$ | | | 877 | | | −68.4 | | | 31.4 |
| $PH_3F_{ap}$ | 721 | 506 | | 347 (F) | 201 | | 12.6 (H) | 24 | |
| | | | | 32 (H) | 31 | | | | |
| $PH_4$ | 519 | 674 | 255 (195)[d] | 199 | 245 | 262 (261)[d] | 6 | 2 | (23)[d] |

[a] Computed using the conversion factors: 3638 G for $^{31}P$, 17 100 G for $^{19}F$, 507 G for $^{1}H$, and the corresponding calculated s orbital spin densities. [b] The experimental and INDO computed results are from ref 53. [c] The 4-31G results are from the present work. [d] Ab initio unrestricted Hartree–Fock calculations which allowed for annihilation of the quartet contribution. The geometry used was TBP-e with all P–H distances set as 1.43 Å. T. A. Claxton, B. W. Fullman, E. Platt, and M. C. R. Symons, *J. Chem. Soc., Dalton Trans.*, 1395 (1975).

INDO calculations and also $SH_2F_2$ with $PH_2F_2$. All methods favor distorted TBP-e structures for these molecules but it appears that the INDO[43] structures for these molecules exaggerate the P–F bond distances when one considers that the present results for $PH_2F_2$ and Gleiter and Veillard's[45] work on $SH_2F_2$ are in rather good agreement. Kutzelnigg[51] also finds using nonempirical calculations an optimized axial PF distance of 1.75 Å in $PH_3F_2$ assuming the PH bonds to be fixed at 1.36 Å. The angles found for $PF_4$ by INDO are in moderately good agreement with our results. It is generally assumed that bond angle variations can lead to large changes in the s character of the odd electron orbital which in turn strongly influences the isotropic hyperfine coupling constants in these radicals.[27]

The Mulliken population analysis[52] as found for structures **9** and **20–22** using the 4-31G wave functions are presented in Table III where we tabulate the s orbital spin densities and the atomic populations. The parenthetic values listed in Table III for $PH_4$ represent the results when d orbitals are admitted to the basis set. It is seen that the d orbitals have the effect of increasing the electron density around phosphorus largely at the expense of the equatorial hydrogens. According to our calculations the electrons in $PH_4$ are much more evenly distributed than in $SH_4$ where Schwenzer and Schaefer[44] find a very uneven electron distribution. The INDO results[43] for $PH_4$ also suggest a larger charge separation but not nearly so large as found for $PH_5$.

An interesting result of the population analysis is revealed by examination of $PF_4$ and $PF_3H$ where it is seen that the equatorial fluorines are in fact more negative than the axial fluorines. This result was also found[43] using INDO wave functions and is contrary to what one finds in the case of pentacoordinate phosphorus where the apical ligand bears the greatest amount of electron density.

For the phosphorane $PX_5$ systems the buildup of charge at the axial ligands is due to the distribution of the HOMO orbital. This doubly occupied molecular orbital places large amounts of electron density at the axial sites rather than the equatorial. We attribute the equatorial fluorines being more negative than the axial for $PF_4$· to the single occupancy of the HOMO. If $PF_4^+$ is calculated in a TBP-e geometry the equatorial fluorines are substantially more negative than the axial. For the $PF_4^-$ system again in a TBP-e geometry the axial ligands are more negative than the equatorial.

In Table IV we compare the experimental[53] and theoretical hyperfine interaction constants for $PH_4$ and the fluorophosphoranyl radicals. The computed hfs constants were obtained from the equation

$$A_{iso} = Q_s\rho_s$$

where $Q_s$ is 3638 G for $^{31}P$, 17 100 G for $^{19}F$, and 506 G for the proton and $\rho_s$ is the SCF spin density computed by INDO[43] or 4-31G. It should be pointed out however that the use of this equation to compute hfs constants is not without criticism.[54] Quantitatively, the results of both molecular orbital methods are not very good. This is especially true of the INDO method which predicts a larger $^{31}P$ hfs constant in $PH_4$ relative to $PF_4$, whereas experimentally the interaction constant in $PF_4$ and its derivatives is over twice as large as that found in radicals derived from $PH_4$. The 4-31G method shows a much more realistic s orbital population on phosphorus in the odd electron orbital in $PH_4$ and $PF_4$. A better quantitative agreement between theory and experiment would probably be forthcoming if the 4-31G wave function, which is not a pure doublet, were purified using the projection operator technique.[55]

It is also interesting to observe that the 4-31G wave function predicts the axial and equatorial hydrogen hfs to have opposite signs in the radicals $PH_4$ and $PH_2F_2$ in agreement with the

experimental ESR observation of Krusic and Meakin[25] for the $t$-$BuOPH_3$ radical.

Further examination of Table IV reveals that there is a monotonic decrease in the experimental $^{31}P$ hfs constant as fluorines are successively replaced by hydrogens in the $PH_nF_{4-n}$ series of radicals. Unfortunately, no experimental results were obtained for $PH_2F_2$, but a comparison of the experimental $^{31}P$ hfs constants with the values computed using 4-31G s orbital spin densities is in fair quantitative agreement and follows the qualitative trend alluded to above; even this qualitative trend is not realized when using the INDO wave functions.

Concluding the discussion of spin densities we are in agreement with the results of Gillbro and Williams[26] where they find for $POCl_3^-$ large spin densities in the $3p_\sigma$ orbitals of the axial chlorines. We find similar large spin densities in the corresponding fluorine orbitals in the radicals **20–22.** In general, for the $PH_nF_{4-n}$ radicals the unpaired electron is largely distributed over the $\sigma$ orbitals of the axial ligands with little spin density residing on the equatorial ligands.[56]

**Acknowledgment.** We are grateful for valuable discussions with Professors R. Hoffmann of Cornell and W. Bentrude of the University of Utah. Mr. L. Kirschenbaum of Brooklyn College kindly performed some of the early calculations. J.M.H. is appreciative of a Faculty Research Award Grant from CUNY.

## References and Notes

(1) (a) Brooklyn College; (b) Staten Island Community College.
(2) (a) J. W. Linnett, "The Electronic Structure of Molecules", Methuen and Co., London, 1964, p 122; (b) R. J. Gillespie and R. S. Nyholm, *Q. Rev., Chem. Soc.*, **11**, 339 (1957).
(3) F. A. Cotton, *J. Chem. Phys.*, **35**, 228 (1961).
(4) R. E. Rundle, *J. Am. Chem. Soc.*, **85**, 112 (1963); *Surv. Prog. Chem.*, **1**, 81 (1963).
(5) (a) E. L. Muetterties and R. A. Schunn, *Q. Rev., Chem. Soc.*, **20**, 245 (1966); (b) E. L. Muetterties, *Acc. Chem. Res.*, **3**, 266 (1970).
(6) (a) L. S. Bartell and K. W. Hansen, *Inorg. Chem.*, **4**, 1777 (1965); (b) L. S. Bartell, *J. Chem. Educ.*, **45**, 754 (1968).
(7) J. I. Musher, *Science*, **141**, 736 (1963); (b) *Angew. Chem.*, **81**, 68 (1969).
(8) J. M. Letcher and J. R. Van Wazer, *J. Chem. Phys.*, **45**, 2916, 2927 (1966).
(9) P. C. Van der Voorn and R. S. Drago, *J. Am. Chem. Soc.*, **88**, 3255 (1966).
(10) D. P. Santry and G. A. Segal, *J. Chem. Phys.*, **47**, 158 (1967).
(11) R. S. Berry, M. Tamres, C. J. Ballhausen, and H. Johansen, *Acta Chem. Scand.*, **22**, 231 (1968).
(12) R. D. Brown and J. B. Peel, *Aust. J. Chem.*, **21**, 2605, 2617 (1968).
(13) D. B. Boyd, *J. Am. Chem. Soc.*, **91**, 1200 (1969).
(14) R. S. Berry, *J. Chem. Phys.*, **32**, 933 (1960).
(15) I. Ugi and F. Ramirez, *Chem. Br.*, **8**, 198 (1972), and references cited therein.
(16) J. B. Florey and L. C. Cusachs, *J. Am. Chem. Soc.*, **94**, 3040 (1972).
(17) K. Issleib and W. Grundler, *Theor. Chim. Acta*, **8**, 70 (1967).
(18) R. Hoffmann, J. M. Howell, and E. Muetterties, *J. Am. Chem. Soc.*, **94**, 3047 (1972).
(19) A. Rauk, L. C. Allen, and K. Mislow, *J. Am. Chem. Soc.*, **94**, 3035 (1972).
(20) A. Strich and A. Veillard, *J. Am. Chem. Soc.*, **95**, 5574 (1973).
(21) (a) J. M. Howell, *Chem. Phys. Lett.*, **25**, 51 (1974); (b) J. M. Howell, J. R. Van Wazer, and A. R. Rossi, *Inorg. Chem.*, **13**, 1747 (1974); (c) J. M. Howell, *J. Am. Chem. Soc.*, **97**, 3930 (1975).
(22) (a) G. M. Whitesides and H. G. Mitchell, *J. Am. Chem. Soc.*, **91**, 5384 (1969); (b) R. R. Holmes, R. M. Dieters, and J. A. Golen, *Inorg. Chem.*, **8**, 2612 (1969).
(23) W. G. Bentrude, "Free Radicals", Vol. 2, J. K. Kochi, Ed., Wiley-Interscience, New York, N.Y., 1973, and references cited therein.
(24) R. W. Fesenden and R. H. Schuler, *J. Chem. Phys.*, **45**, 1845 (1966).
(25) (a) P. J. Krusic, W. Mahler, and J. K. Kochi, *J. Am. Chem. Soc.*, **94**, 6033 (1972); (b) P. J. Krusic and P. Meakin, *Chem. Phys. Lett.*, **18**, 347 (1973).
(26) T. Gillbro and F. Williams, *J. Am. Chem. Soc.*, **96**, 5032 (1974).
(27) J. Higuchi, *J. Chem. Phys.*, **50**, 1001 (1969).
(28) G. B. Watts, D. Griller, and K. U. Ingold, *J. Am. Chem. Soc.*, **94**, 8784 (1972).
(29) A. G. Davies, D. Griller, and B. P. Roberts, *J. Chem. Soc., Perkin Trans. 2*, 993 (1972).
(30) (a) W. G. Bentrude, P. F. Rusek, and J. H. Hargis, *Chem. Commun.*, 5296 (1969); (b) W. G. Bentrude and R. A. Wielesek, *J. Am. Chem. Soc.*, **91**, 2406 (1969); (c) W. G. Bentrude, W. A. Khan, M. Murakami, and H.-W. Tan, *ibid.*, **96**, 5566 (1974); (d) W. G. Bentrude and T. B. Min, *ibid.*, **97**, 2918 (1975).
(31) C. A. McDowell, K. A. R. Mitchell, and P. Raghunathan, *J. Chem. Phys.*, **57**, 1699 (1972).
(32) A. J. Colussi, J. R. Morton, and K. F. Preston, *J. Chem. Phys.*, **62**, 2004 (1975).
(33) H. W. Tan and W. G. Bentrude, *J. Am. Chem. Soc.*, **96**, 5950 (1974).
(34) Penkovsky using CNDO/2 finds the TBP → SP isomerization for $PF_5$ to cost 5 kcal/mol, while the same change for $PF_4$ costs 25 kcal/mol; personal communication, W. G. Bentrude.
(35) Recent results by S. P. Mishra and M. C. R. Symons, *Chem. Commun.*, 279 (1974), question the previously accepted mobility of ligands in $PF_4$ demonstrated by J. R. Morton, *Can. J. Phys.*, **41**, 706 (1963).
(36) W. G. Bentrude and T. B. Min, *J. Am. Chem. Soc.*, **94**, 1025 (1972).
(37) C. A. Coulson, *Nature (London)*, **221**, 1106 (1969).
(38) Program available from Quantum Chemistry Program Exchange (No. 236), Chemistry Department, Indiana University, Bloomington, Ind.
(39) (a) W. J. Hehre, R. F. Stewart, and J. A. Pople, *J. Chem. Phys.*, **51**, 2657 (1969); (b) R. Ditchfield, W. J. Hehre, and J. A. Pople, *ibid.*, **54**, 724 (1971); W. J. Hehre and W. A. Lathan, *ibid.*, **56**, 5255 (1972).
(40) POLYATOM (version 2), QCPE program No. 199, Indiana University, Bloomington, Ind.
(41) J. A. Pople and R. K. Nesbet, *J. Chem. Phys.*, **22**, 571 (1954).
(42) J. M. F. Van Dijk, J. F. N. Pennings, and H. M. Buck, *J. Am. Chem. Soc.*, **97**, 4836 (1975).
(43) A. J. Colussi, J. R. Morton, and K. F. Preston, *J. Phys. Chem.*, **79**, 651 (1975).
(44) G. M. Schwenzer and H. F. Schaefer III, *J. Am. Chem. Soc.*, **97**, 1391 (1975).
(45) R. Gleiter and A. Veillard, *Chem. Phys. Lett.*, in press; see also M. Chen and R. Hoffmann, *J. Am. Chem. Soc.*, **97**, 1647 (1975).
(46) The energies for the "doubly occupied" orbitals are an average of the values for the $\alpha$ and $\beta$ spin orbitals. For the odd electron orbital the $\alpha$ value is used. The PH distance was constrained to 1.558 Å.
(47) R. G. Pearson, *J. Am. Chem. Soc.*, **91**, 4947 (1969); *Proc. Natl. Acad. Sci. U.S.A.*, **72**, 2104 (1975).
(48) L. S. Bartell and R. M. Gavin, *J. Chem. Phys.*, **48**, 2466 (1968).
(49) J. I. Musher and A. H. Cowley, *Inorg. Chem.*, **14**, 2302 (1975).
(50) L. Radom and J. A. Pople, *MTP Int. Rev. Sci.: Theor. Chem.*, **1**, 78 (1972).
(51) F. Keil and W. Kutzelnigg, *J. Am. Chem. Soc.*, **97**, 3623 (1975).
(52) R. S. Mulliken, *J. Chem. Phys.*, **23**, 1833, 1841 (1955).
(53) A. J. Colussi, J. R. Morton, and K. F. Preston, *J. Phys. Chem.*, **79**, 1855 (1975).
(54) Y. I. Gorlov, I. I. Ukrainsky, and V. V. Penkovsky, *Theor. Chim. Acta*, **34**, 31 (1974).
(55) J. E. Harriman, *J. Chem. Phys.*, **40**, 2827 (1964).
(56) K. Nishikida and F. Williams, *J. Am. Chem. Soc.*, **97**, 5462 (1975).